

Metabolic oxygen consumption measurement with a single-cell biosensor after particle microbeam irradiation

Yanping Xu · Bo Zhang · Mark Messerli ·
Gerhard Randers-Pehrson · Tom K. Hei ·
David J. Brenner

Received: 19 March 2014 / Accepted: 9 October 2014 / Published online: 22 October 2014
© Springer-Verlag Berlin Heidelberg 2014

Abstract A noninvasive, self-referencing biosensor/probe system has been integrated into the Columbia University Radiological Research Accelerator Facility Microbeam II end station. A single-cell oxygen consumption measurement has been conducted with this type of oxygen probe in 37° C Krebs–Ringer Bicarbonate buffer immediately before and after a single-cell microbeam irradiation. It is the first such measurement made for a microbeam irradiation, and a six fold increment of oxygen flux induced during a 15-s period of time has been observed following radiation exposure. The experimental procedure and the results are discussed.

Keywords Ionizing radiation · Microbeam · Bystander effect · Biosensor · Radiation sensitivity

Introduction

Charged particle microbeams have been significant contributions to define the biological targets of ionizing radiations.

Y. Xu (✉) · G. Randers-Pehrson · D. J. Brenner
Radiological Research Accelerator Facility (RARAF), Center for
Radiological Research, Columbia University, 136 S. Broadway,
Irvington, NY 10533, USA
e-mail: yx2132@columbia.edu

B. Zhang · T. K. Hei
Center for Radiological Research, Columbia University,
New York, NY 10032, USA

M. Messerli
Biocurrents Research Center, Marine Biological Laboratory,
Woods Hole, MA 02543, USA

M. Messerli
Department of Biology and Microbiology, South Dakota State
University, Brookings, SD 57007, USA

They established cell nuclear and cytoplasmic responses of targeted cells, along with responses of nontargeted bystander cells (Hei et al. 2009). There is evidence that radiation-induced bystander signals between cells may originate with a diffusible mediator (Shao et al. 2002; Matsumoto et al. 2001; Azzam et al. 2002). To physically demonstrate the radiation-induced oxygen flux changes outside the irradiated cell, a self-referencing amperometric electrochemical sensor was proposed for use with single-cell irradiation experiment. This type of micro-biosensor allows sensitive and noninvasive measurement of the flux of radical mediators, such as oxygen (or nitric oxide), in single cells. This is achieved by repeatedly moving the micro-biosensor/probe tip through the extracellular gradient at a known frequency and between points a known distance apart (Fig. 1). This so-called self-referencing technique minimizes the measurement challenges caused by the random drift of the sensor output. In conjunction with a microbeam, it has the capacity to accurately detect selected ionic and molecular gradient changes surrounding a single cell with high spatial resolution. Our first radiobiology experiment was to analyze metabolic oxygen consumption in individual living lung cell after subcellular irradiation and to explore the radiation response of such cells. The self-referencing oxygen electrochemical system was developed at the BioCurrents Shared Resource at the Marine Biological Laboratory (MBL), Woods Hole, MA. It was integrated with the Radiological Research Accelerator Facility (RARAF) single-particle, single-cell microbeam to form a single-cell irradiation response detection platform.

Microbeam

A microbeam is an irradiation system which delivers a certain number of particles with a micron-sized diameter

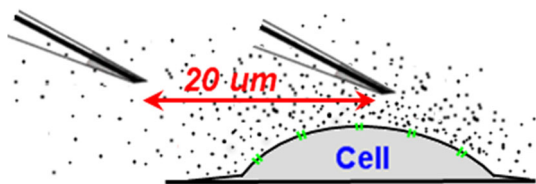


Fig. 1 Measuring oxygen flux with micro-biosensor

spot to a chosen biological target, which allows damage to be precisely deposited within specific locations (e.g., nuclei or cytoplasm of single cells). The RARAF microbeam is driven by a 5.5 MV HVEE Singletron Accelerator. The particles are ionized by a radio frequency (RF) ion source inside the Singletron Accelerator and are accelerated from a DC high voltage terminal to reach the desired energy. Then, the particle beam passes through a beam transport system to the beam end station where irradiation experiments take place. The beam transport system includes a few beam manipulation elements (Fig. 2). The main beam slits and beam stop are used to eliminate unwanted ion beams, to limit the size of the beam entering a 90-degree bending magnet and to stop the beam from entering the bending magnet when irradiations are not expected. The magnetic steering magnet is used to make fine adjustments aiming the ion beam at the entrance of the bending magnet. The 90-degree bending magnet is used to bend the beam into the vertical direction. The beam deflector/shutter is an electrostatic system that steers the beam rapidly (~ 1 ms) to end the irradiation of a cell. The object aperture (~ 30 μm diameter) limits the initial beam size. A custom-built electrostatic double-quadrupole triplet system (Porterfield et al. 2001) is used to focus the beam at the position of the cells to be irradiated. In front of the first triplet lens, an angular limiting aperture is used to eliminate particles

entering at large angles to help reduce the diameter of the beam spot. The beam exit window is a thin silicon nitride foil attached to a stainless steel disk, with thickness of either 500 or 100 nm (for a sub-micron beam spot) to minimize scattering of the beam. The cell dish holder is designed to locate cells at the focusing plane of the microbeam and is in the view range of a customized microscope. An imaging/targeting system comprises a precision XYZ stage (MadCity Labs, Inc. WI), a Nikon Eclipse E600 microscope and an attached PhotonMAX-512B EMCCD camera (Princeton Instruments, NJ). This equipment combination also allows us to image the wide range of fluorescent proteins that have been developed. A computer control program written in Visual Basic locates the cells, plated in a cell culture dish, and positions them for irradiation. While the RARAF microbeam is primarily used for charge particle irradiation, the accelerator can be used as a source for neutral particle radiation, e.g., neutron radiation (Xu et al. 2011, 2012).

Oxygen self-referencing micro-biosensor

Self-referencing polarographic (*SERP*) microsensor technology was developed at the BioCurrents Shared Resource (Land et al. 1999; Porterfield et al. 2001; Kumar et al. 2001). These sensors are made of borosilicate glass capillaries (1B150, WPI) which are pulled to outer tip diameters of ~ 3 μm using a Sutter P-97 (Sutter Instrument, CA). Then, a 25- μm -diameter gold wire (Alfa Aesar, Ward Hill, MA) is electrochemically etched in an aqueous solution of 1N HCl to reduce the tip diameter to ~ 1 μm . After being rinsed with water and isopropyl alcohol, the etched Au wire is inserted into the capillary so that the wire protrudes slightly from the pipette tip. The electrode tip is dipped into

Fig. 2 RARAF microbeam

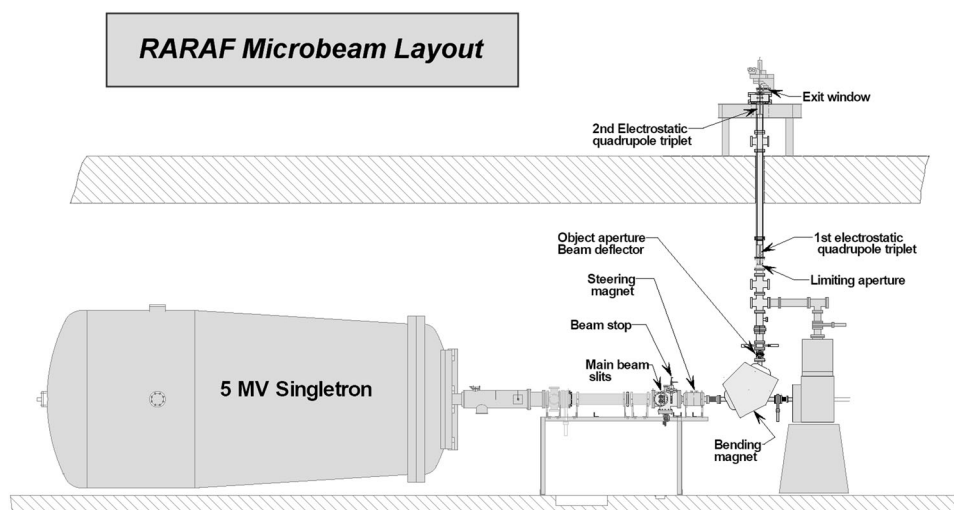
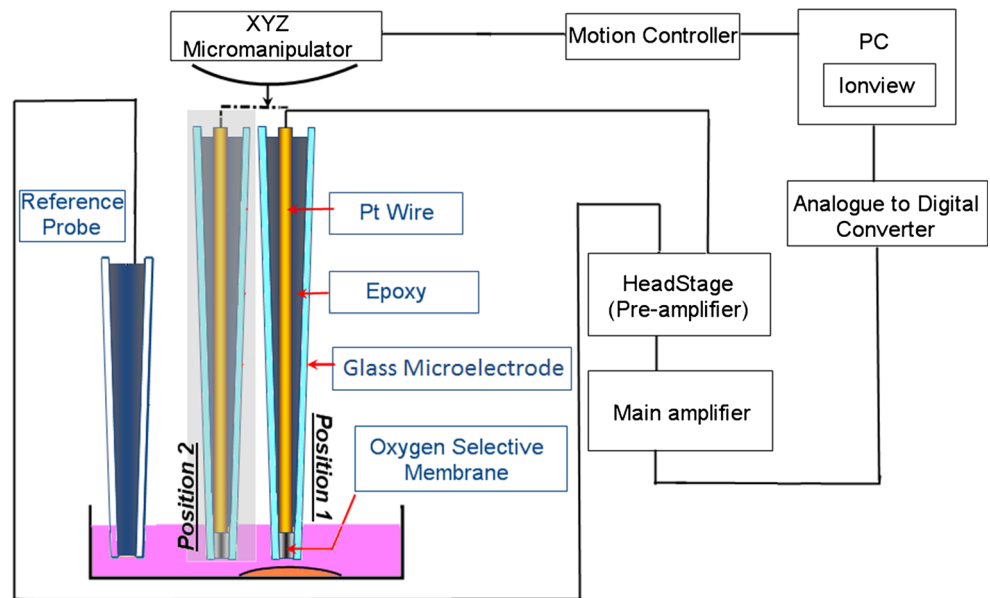


Fig. 3 Self-referencing micro-biosensor detection system

UV curing epoxy (429, Dymax, Torrington, CT). The exposed Au electrode is then etched again (same conditions as above) to form a recessed electrode with a cavity 2–3 μm deep. Finally, the electrode is coated by dipping it in a solution of 10 % cellulose acetate (30 kDa) for 60 s and drying for 5–10 min. The electrochemical sensor itself is attached to a BRC amperometric head stage via a modified BNC connector. An L-shaped Ag/AgCl reference electrode, connected via a 3M KCl/5 % agar bridge (reference probe) placed in the bulk solution, completes the circuit (Fig. 3). Selectivity for amperometric electrodes is usually defined by the conditioning, operating voltage and excluding membranes. For oxygen detection, the electrodes are polarized to -0.6 V. They have a rapid response time and are normally used at a modulation frequency of 0.3 Hz and moved over a distance of 10–20 μm . The relationship between oxygen concentration and the current signal from an electrode being oscillated within an oxygen gradient is:

$$C_1 - C_2 = (SI_1 + b) - (SI_2 + b) \quad (1)$$

where I is the electrode output, C is the oxygen concentration and S is the slope of the electrode calibration and b is the y -intercept of the electrode calibration. Writing this equation as $\Delta C = S \Delta I$, ΔC can be reconciled with the amplitude of electrode oscillation, Δr , using the Fick equation to obtain a measurement of the oxygen flux:

$$J = -DS(\Delta I/\Delta r) \quad (2)$$

where J is the diffusion flux and D is the diffusion coefficient. The *SERP* microsensors operate on platforms very similar to standard electrophysiological setups.

System integration

For single-cell irradiation response measurements, sensor access during and after irradiation for precision location of damage within single cells with the imaging system is crucial. Microprobe measurements without irradiation are usually performed on an inverted microscope giving open access from above for probe placement. With microbeam irradiation, there is a constraint from the exit window below the sample, so microscopy and probing must be done from above the sample. Access requires that the tip of the probe (microelectrode) approaches a single cell, at an angle of between 20° to 30° , to within microns of the plasma membrane. Access for the reference electrode is also required. Both the measuring probe and the reference electrode have body diameters of 1.5 mm, while the measuring tip is drawn to a point. A Nikon 10 \times long working distance (4 mm) dry microscope objective is placed with the probe in a sample dish. Because the probe approach angle is so severely constricted, the angle-setting technique appropriate for an open access system is completely inadequate. An offset hinge manipulator was designed (Fig. 4) and built which allows rapid repeatable repositioning of the probe and simple angle adjustments. The hinge was constructed in a stacked configuration using high-precision flex pivots in such a way that angular settings between 10 and 60° can be set. In order to use the manipulator and the stacked hinge to satisfy our needs, a universal mounting car (Thorlabs, NJ) riding on an optical rail with an integrated robotic retraction mechanism is used. The probe manipulators are mounted accurately on the car for simple interchange. This robotic manipulator structure and the associated fully integrated control systems allow us to

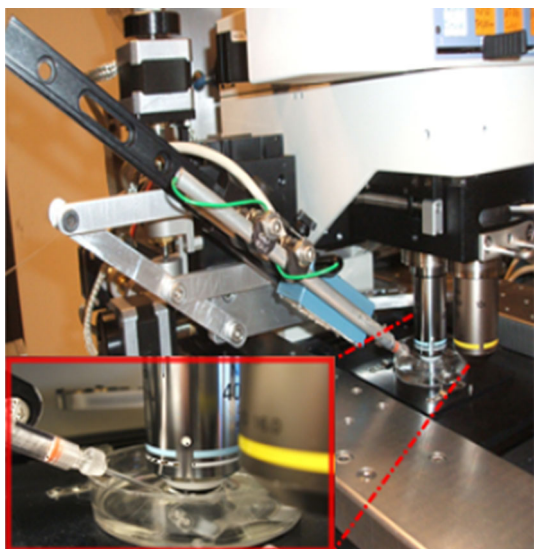


Fig. 4 Electrochemical microsensor mounted on microbeam end station by the offset hinge system

meet all the micromanipulation and capillary probe placement needs in an efficient manner.

Measurement

Cell preparation

The first step of experiment was preparing the cell samples. The human telomerase reverse transcriptase (hTERT) immortalized human small airway epithelial (SAE) cells were thawed from liquid nitrogen and cultured in fresh medium. Cells were diluted in fresh medium so that a select number of cells were contained in 10 ml of medium. Cultured cells were maintained at 37 °C in a humidified 5 % CO₂ incubator overnight. The microbeam cell culture dishes were custom-made for cell growth and cell irradiation. They are made of 60-mm Falcon Petri dish, and a 0.25-inch-diameter hole is drilled into the center of the dish bottom. The polypropylene film covered on the bottom of microbeam dish wells was treated with Cell-Tak (BD Biosciences) to enhance cell attachment. Polypropylene was chosen because it is nonfluorescent, and also, this thin polypropylene allows the chosen radiation to get through to the cells while allowing them to be placed upright on the microbeam end stations with minimal distance between the dish bottom and beam exit window. Dishes were incubated at 37 °C for 30 min and were then rinsed. In the next step, the cells were trypsinized and diluted to 1.5×10^4 /ml (about 30 cells in a total volume of 2 μ l medium). A sterile 18- to 22-mm square coverslip covered the well after cells in a droplet were plated using a micropipetter as close as possible to the center of the dish. The dishes were placed in an incubator until cells get

attached to the polypropylene. After cell attachment, the coverslips were removed and an additional 5 ml of medium was replenished to the dishes. Cells will typically flatten out within 1–3 h. The cells were stained by exposure to a 50 nM solution of the vital DNA-binding stain Hoechst 33342 for 30 min prior to radiation. This low stain concentration necessitates the use of an EMCCD camera (Princeton Instrument) to obtain a high-contrast image and allows rapid location of the cell nuclei to be hit, or not hit, as the experiment calls for during irradiation.

Radiation beam setup

Beam size and beam location were measured with a nickel knife edge scan (Randers-Pehrson et al. 2009). Beam location was registered using scanning of fluorescent beads. This was done by placing a microbeam dish containing fluorescent beads on the stage. Then, an isolated bead was moved to the approximate beam position. A spiral energy loss mapping scan was conducted with a solid state charge particle detector. Once the center of the beam was identified, the bead was moved to that position (the center of beam mapping), and the beam location was registered with the imaging system. The low-magnification pictures of the bead were taken, and a center-of-gravity program routine was used to transfer the bead coordinates to the computer.

Biosensor/Prober setup

The cell dish was removed from incubator and was mounted on the microbeam stage. The chosen cell was moved to the registered beam position with an XYZ stage (MadCity Labs, Inc. WI) while monitored with a Nikon Eclipse E600 microscope, and a reference picture was taken with an attached PhotonMAX-512B EMCCD camera. Then, the micro-electrochemical sensor and reference electrode were mounted on the BioCurrents XYZ stage (Newport, CA), and the sensor/probe was carefully moved close to the cytoplasm (about 10–15 μ m away) monitored with a Nikon 10 \times lens, and a background/control measurement was run for about 30 min with the sensor moved rapidly between two positions 15 μ m apart at a frequency of 0.3 Hz (Fig. 5). Data were collected at each pole position for approximately 1 s or 70 % of the cycle time. The tip of a sensor is shown (Fig. 6) near a source of the analyte. The current signals were averaged at each position, then a differential current was obtained that can be converted into a directional measurement of flux using the Fick equation. Referencing the signals in this manner has the advantage that sources of interference caused by random drift and noise are effectively filtered from the signal and fluxes can be monitored in real time. The probe was in

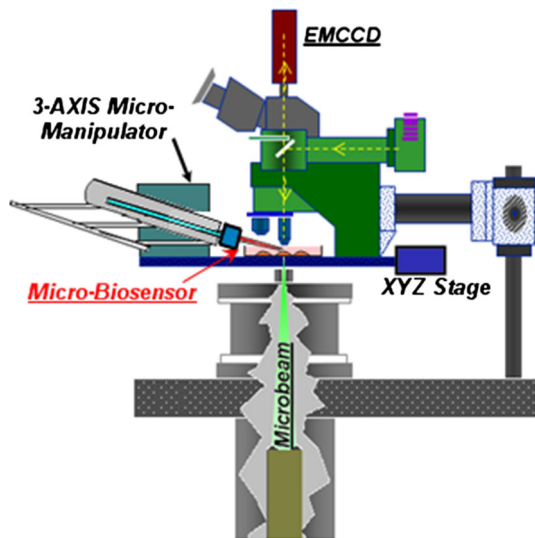


Fig. 5 Measurement setup on microbeam end station

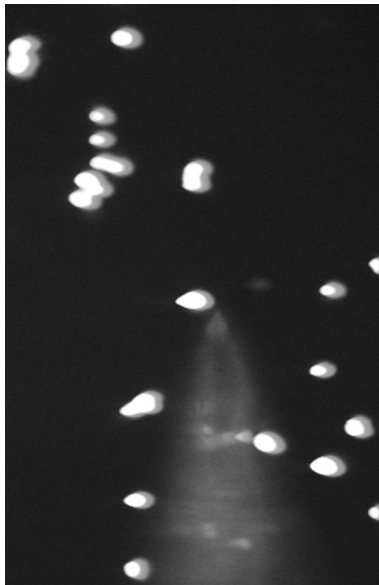


Fig. 6 Biosensor/probe imaging with the cell

equilibrium after the 30-min preprocess period, and the measured background data were logged in the control computer.

Radiation and real-time oxygen consumption measurement

The next step was the single-cell microbeam irradiation with monitoring of the current changes in self-referencing mode. The number of helium ions was set at 20 or 30 in the microbeam irradiation protocol for this single-cell irradiation. The particle beam count rate was measured at about 200

per second. A pulser (Ortec Inc, TN) was used to simulate the real count rate and to control the beam shutter, because the 5.6 MeV helium ions cannot pass all the way through the cell and the medium (~ 1 mm thick) without being absorbed. In the cytoplasm irradiation experiments, an exclusion zone around each fluorescing nucleus is automatically generated to ensure that the cytoplasm target positions from one cell are not accidentally within the nucleus of an adjacent cell. Mutation induction caused by cytoplasmic irradiation has been reported using this technique. The image analysis system defines the long axis of each cell nucleus, after which the computer system delivers particles at two target positions along this axis, $6 \mu\text{m}$ away from each end of the cell nucleus. During the experiment, an in-house code with Matrox Genesis imaging library has been used to handle the images (subtract background, correct for illumination variation, locate cells, and record location of nearest frame).

Results and discussion

Five freshly made oxygen electrodes were pretested for this experiment. They were all held at -0.6 V (DC), and the current decreased to nearly zero when the electrode was placed in a solution without oxygen at room temperature. DC and AC currents were separately measured for each probe over a 30 min period. It was found that three probes (#1, #4 and #5) produced consistent DC currents and rapidly moderately spiking AC currents (Fig. 7). Two probes (#2 and #3) displayed rapid large current declines and were considered unsuitable for further use. The recordings were made at 37°C in KRB buffer, which matches our microbeam buffer in complexity. Probe #1 has the lowest DC current and the lowest noise when held at -0.6 V. It can still measure O_2 changes by clamping the voltage to -0.7 V. Some probes, e.g., Probe #4 and probe #5, needed more than 30 min to get to equilibrium, and their noise is a bit higher. Normally, the probes require at least 20 min to reach equilibrium.

Glass beads $20 \mu\text{m}$ in diameter were used for positioning tests, and they interfered with O_2 diffusion to the sensor. The electrode can detect this when the current is high enough. The noise of a good O_2 electrode is usually <60 fA peak-to-peak. In real cell measurements, O_2 flux varies from cell-to-cell based on cellular and mitochondrial activity and size. For small single cells, the O_2 flux gives rise to AC currents between 10 and 100 fA over a 10 – $20 \mu\text{m}$ distance next to the cell surface. If the electrode is damaged, the current from that electrode will be too high. On the other hand, about $\sim 30\%$ of electrodes coated became noisy again simply by sitting in the container, possibly due to the oxygen permeable membrane on the tip drying out, becoming dislodged or coming removed in solution. The oxygen permeable

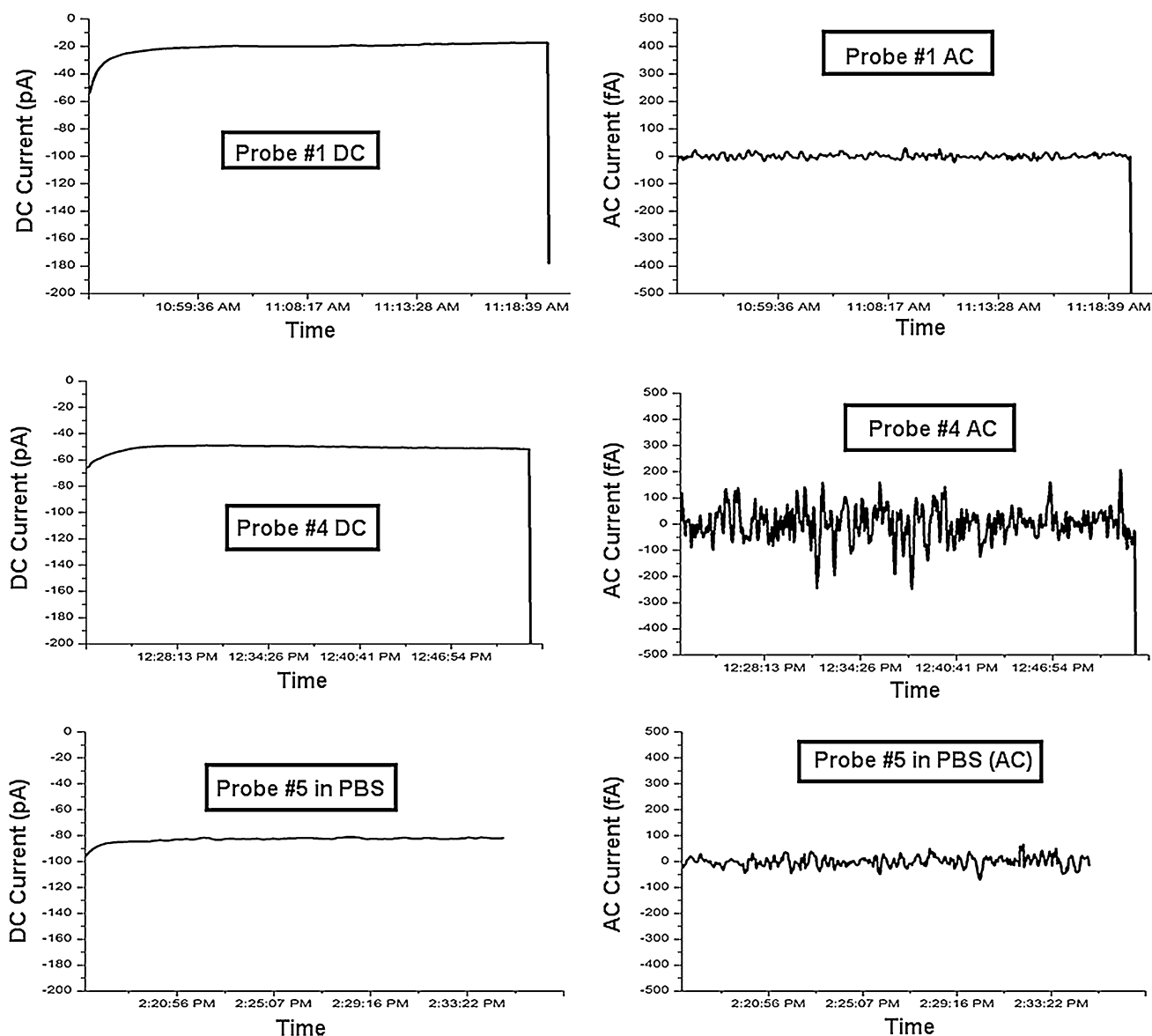


Fig. 7 Self-referencing oxygen-selective probe testing result without irradiation

membrane simply helps ensure that oxygen diffusion to the tip is the rate-limiting step for oxygen reduction. Cellulose acetate is applied in an organic solvent so it is absolutely dry before it is placed in aqueous solution. However, it becomes hydrated relatively well. Overtime, it may become dislodged or come off especially at warmer temperatures. Dip coating them again on the day before experiment fixed the problem.

Human lung cells were used in this single-cell irradiation experiments. To detect physiologically driven molecular movements around the cell membrane, which is normally very small (fA current), the drift and background have to be taken care of with self-referencing technique. This requires extracting small electrical signals, fA differences (AC) on top of large offset signals 10s of pA

(DC). With cells exposed to 10 μ M antimycin, we tested the basal cellular O_2 flux and detected changes in oxygen-concentration-dependent current (DC changes). Then, we conducted both cytoplasm and nucleus irradiations with 100 % cell radiation. Figure 8 shows the background and drifting (DC) during the radiation. A very obvious O_2 current change (AC) was recorded within seconds after cytoplasm irradiation. Figure 9 shows the AC current change from two measurements with two different probes. The small changes in oxygen consumption could be extracted from the background oxygen concentration with the self-referencing method. A similar but relatively small change was observed after nucleus irradiation. Without radiation, we did not see any of these large spikes on a long-time background measurement.

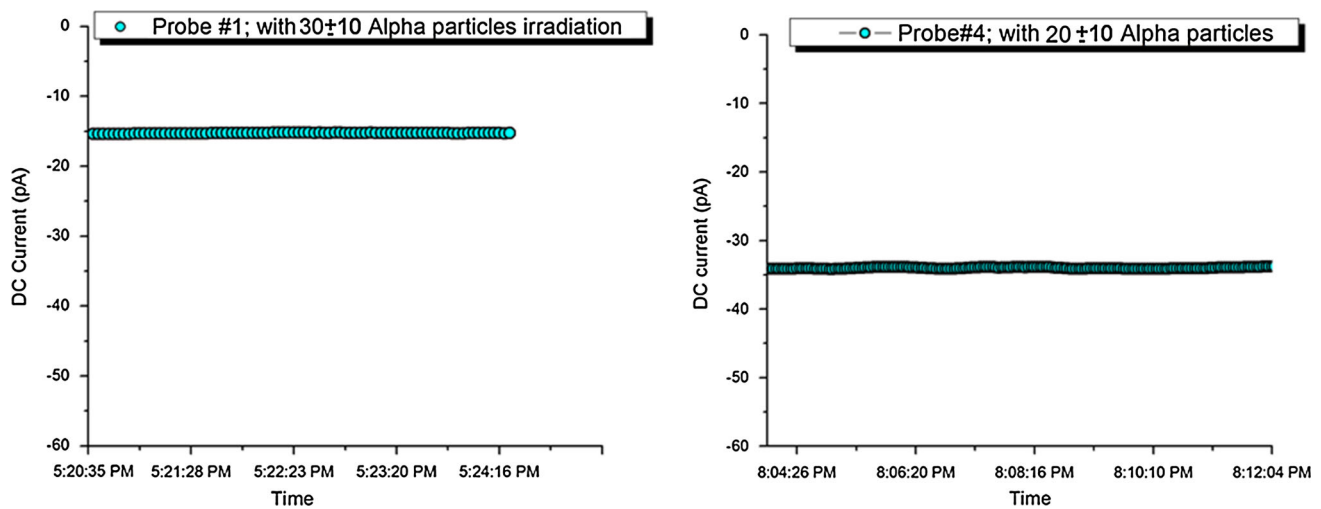


Fig. 8 Self-referencing oxygen ion-selective probe result with Alpha microbeam irradiation (DC)

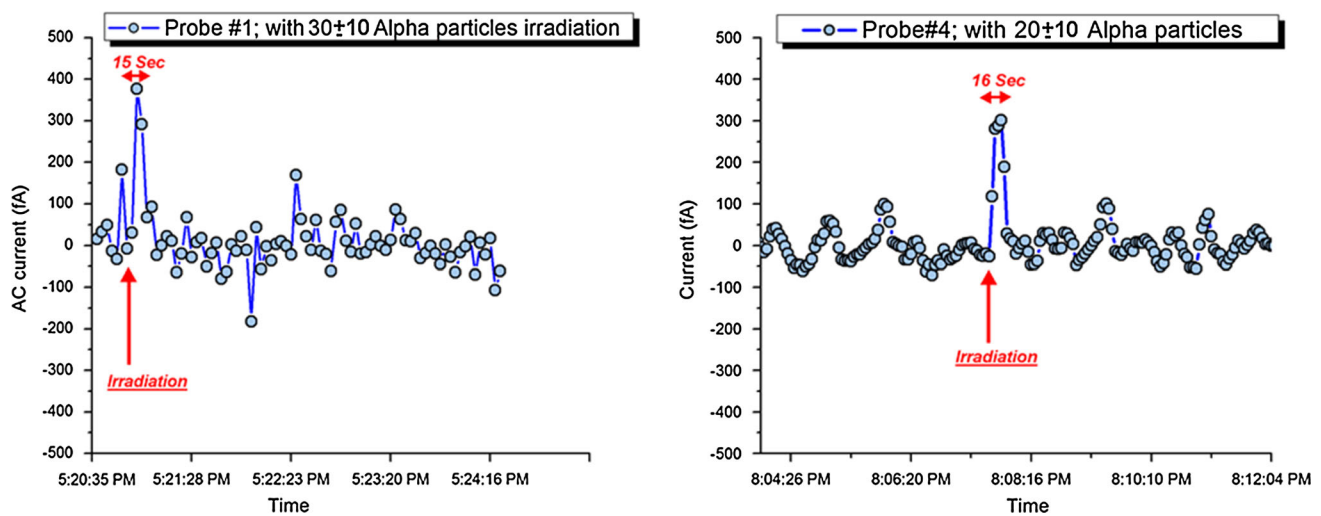


Fig. 9 Self-referencing oxygen ion-selective probe result with Alpha microbeam irradiation (AC)

This is the first time a physiological experiment on individual cells was performed to assess the oxygen current change associated with a radiation exposure. Twelve measurements were conducted resulting in a success rate of $\sim 30\%$ as determined by the individual cell flux test because of the cell-to-cell variations and the uncertainty of the probe locations. Only successfully measured data are subsequently analyzed.

This study demonstrates a novel, real-time radiobiology analysis through integrating a biosensor into the microbeam system to explore physiological responses after single-cell irradiation. The results indicate a role for mitochondrial damage following irradiation and enable further evaluations of the radiation-induced bystander effect. This effect is hypothetically due to the result of damage signals received by non-hit cells from hit cells.

Establishing the mechanistic basis for such responses in the form of damage signaling from hit to non-hit cells and continued signaling has proven to be elusive. However, evidence for both oxygen- and nitrogen-based small molecules and mitochondrial dysfunction has been produced. The approach outlined in this study suggests that biosensor mediators in the form of oxygen radicals, nitric oxide and hydrogen peroxide can be directly measured at a single-cell level in both hit cells and bystander cells providing an incisive method of evaluating such evidence. This establishment of a noninvasive, self-referencing biosensor/probe system in conjunction with the RARAF microbeam provides an additional means for probing biological responsiveness at the level of individual cell, after precise subcellular targeting in hit cells and bystander cells.

Acknowledgments We thank Dr. Alan Bigelow and Professor Charles Geard for their helpful discussions of the experiment and the results. This work was supported by the National Institute of Biomedical Imaging and Bioengineering (NIBIB grant P41EB002033) and by funding from the National Cancer Institute (NCI P01-CA49062-22).

References

- Azzam EI, de Toledo SM, Spitz DR and Little JB (2002) Oxidative metabolism modulates signal transduction and micronucleus formation in bystander cells from alpha-particle-irradiated normal human fibroblast cultures. *Cancer Res* 62:5436–5442
- Hei TK, Ballas LK, Brenner DJ, Geard CR (2009) Advances in radiobiological studies using a microbeam. *J Radiat Res* 50: A7–A12. doi:[10.1269/Jrr.08135s](https://doi.org/10.1269/Jrr.08135s)
- Kumar SM, Porterfield DM, Muller KJ, Smith PJS, Sahley CL (2001) Nerve injury induces a rapid efflux of nitric oxide (NO) detected with a novel NO microsensor. *J Neurosci* 21:215–220
- Land SC, Porterfield DM, Sanger RH, Smith PJS (1999) The self-referencing oxygen-selective microelectrode: detection of transmembrane oxygen flux from single cells. *J Exp Biol* 202:211–218
- Matsumoto H, Hayashi S, Hatashita M, Ohnishi K, Shioura H, Ohtsubo T, Kitai R, Ohnishi T, Kano E (2001) Induction of radioresistance by a nitric oxide-mediated bystander effect. *Radiat Res* 155:387–396. doi:[10.1667/0033-7587\(2001\)155\[0387:Iorban\]2.0.Co;2](https://doi.org/10.1667/0033-7587(2001)155[0387:Iorban]2.0.Co;2)
- Porterfield DM, Laskin JD, Jung SK, Malchow RP, Billack B, Smith PJS, Heck DE (2001) Proteins and lipids define the diffusional field of nitric oxide. *Am J Physiol Lung C* 281:L904–L912
- Randers-Pehrson G, Johnson GW, Marino SA, Xu YP, Dymnikov AD, Brenner DJ (2009) The Columbia University sub-micron charged particle beam. *Nucl Instrum Methods A* 609:294–299. doi:[10.1016/j.nima.2009.08.041](https://doi.org/10.1016/j.nima.2009.08.041)
- Shao C, Furusawa Y, Aoki M, Matsumoto H, Ando K (2002) Nitric oxide-mediated bystander effect induced by heavy-ions in human salivary gland tumour cells. *Int J Radiat Biol* 78:837–844. doi:[10.1080/09553000210149786](https://doi.org/10.1080/09553000210149786)
- Xu YP, Randers-Pehrson G, Marino SA, Bigelow AW, Akselrod MS, Sykora JG, Brenner DJ (2011) An accelerator-based neutron microbeam system for studies of radiation effects. *Radiat Prot Dosimetry* 145:373–376. doi:[10.1093/Rpd/Ncq424](https://doi.org/10.1093/Rpd/Ncq424)
- Xu Y, Garty G, Marino SA, Massey TN, Randers-Pehrson G, Johnson GW, Brenner DJ (2012) Novel neutron sources at the Radiological Research Accelerator Facility. *J Instrum* 7:C03031. doi:[10.1088/1748-0221/7/03/C03031](https://doi.org/10.1088/1748-0221/7/03/C03031)